

Chapter 27

FUNDAMENTAL INVESTIGATION INTO THE INTERACTIONS AND LIMITATIONS OF PRIMARY DUST CONTROLS FOR CONTINUOUS MINERS

J. F. Colinet, J. J. McClelland, and R. A. Jankowski

Mining Engineer, Mining Engineer, Supervisory Physical Scientist,
Pittsburgh Research Center, U.S. Bureau of Mines, Pittsburgh, PA

Abstract. Laboratory tests were conducted by the U.S. Bureau of Mines to determine the respirable dust reduction effectiveness of and interaction between face airflow and water sprays for a continuous miner. Exhausting face ventilation was varied from 3,000 to 9,000 cfm (1.42 to 4.25 m³/sec). Spray-water-flow was varied from 15 to 35 gpm (0.057 to 0.132 m³/min), while nozzle operating pressure was varied from 80 to 200 psi (5.62 to 14.06 kg/cm²). Results from gravimetric dust samples indicated that airflow had the greatest individual impact on reducing dust levels, with return and operator concentrations reduced by as much as 57% and 99%, respectively.

Interactions between dust control parameters were found to be significant. Often, these interactions defined a level of application for a control parameter where further increases in that parameter failed to produce additional reductions in dust concentrations. In several cases, increases in a control parameter resulted in higher dust levels at the operator's location. These higher dust levels were attributed to additional rollback and/or airflow turbulence. Regression modeling indicated that increases in airflow to 8,400 cfm (3.96 m³/sec), water flow to 25 gpm (0.095 m³/min), and water pressure to 140 psi (9.84 kg/cm²) typically were beneficial at the operator and return sampling locations.

INTRODUCTION

Given the known health-hazards associated with breathing respirable coal and silica (quartz) dust generated during mining, mine operators are continually seeking ways to minimize worker exposure. Ventilation air and water sprays are the primary means used to control dust liberation and worker exposure. Ventilating air dilutes the generated dust and also, carries airborne dust away from workers. Water applied through machine-mounted spray systems suppresses dust entrainment and also, removes dust that has become entrained in the ventilating air. However, the application of

air and water to control dust is not without limit. From an operation viewpoint, increases in these control parameters add to the financial cost of producing coal and at some level, may aggravate other conditions in the mine (wet floor, increased belt wear) or outside the mine (acid mine drainage, increased noise from larger ventilation fans). From a research standpoint, continual increases in these control parameters do not ensure further reductions in dust levels. Thus, the application of these controls should be planned and undertaken with care to maximize effectiveness.

The objective of this program was to determine those levels of air quantity, water quantity, and water pressure that result in the lowest dust levels at the continuous miner operator position and in the return. Information about the interaction between control parameters and maximum effective limits for each parameter were of particular interest.

Laboratory testing was conducted at three different levels for each control parameter. The baseline levels were established at 15 gpm, 80 psi, and 3,000 cfm, while the maximum levels were 35 gpm, 200 psi, and 9,000 cfm. This report summarizes respirable dust sampling results obtained for combinations of these parameters at various levels. Regression analysis was used to model the dust levels that could be expected within these ranges.

MINE TEST FACILITY

All tests were conducted in the full-scale, simulated mine gallery at the Bureaus' Pittsburgh Research Center. The mine entry was 18 ft (5.49 m) wide with a mining height of 80 in. (2.03 m). The face area simulated a 15 ft (4.57 m) deep box cut, with an approximately 6 ft (1.83 m) wide by 15 ft long slab remaining on the left side of the entry. Figure 1 shows the simulated mine layout as used for this test program.

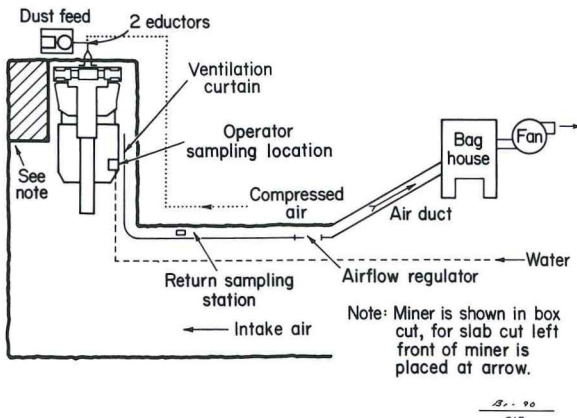


FIGURE 1. Mine test facility.

A full-scale wooden model of a Joy 14 CM continuous miner was used in testing. The miner was positioned within 1 ft of the face in the box cut for a series of box cut tests and subsequently relocated to the left side of the entry within 1 ft of the slab for a series of slab cut tests. The cutter boom of the miner was in a raised position during the first half of each test and then lowered for the second half. The cutting head of the miner was operated throughout all tests.

For this program, the miner was equipped with two spray manifolds. One manifold was mounted on top of the cutter boom, while the second was mounted on the underside of the boom. The top manifold was drilled and tapped to hold 12 spray nozzles, equally spaced across the length of the manifold. The underboom manifold contained 6 equally spaced, spray nozzles. All nozzles produced hollow cone spray patterns and were oriented perpendicular to the face.

Two mini-eductors utilized compressed air at 50 psi (3.52 kg/cm^2) to transport dust through two hoses into the face area of the mine gallery. Both discharge hoses were mounted on the model miner in the area of the ripper chain. One hose discharged in front of the right cutter drum, while the second discharged in front of the left drum. For these tests, a screw feeder supplied approximately 28 grams per minute of feed dust into the eductors. The feed dust was minus 50 micrometers in size and representative of airborne dust found in continuous mining operations (Ramani, Mutmansky, Bhaskar, and Qin, 1987).

An exhaust fan, rated at 20,000 cfm ($9.44 \text{ m}^3/\text{sec}$), provided airflow to the face. An adjustable regulator in the return airway was used to control the quantity of airflow reaching the face for each test.

A totalizing meter and a flow meter were installed in the water supply line to the miner. The totalizing meter was utilized to obtain an

average water flow rate in gallons per minute. For each test, the total gallons, calculated from readings taken at the beginning and end of each test, were divided by the test time to obtain the average flow rate. The flow meter provided a real-time, flow measurement in the form of an electrical output that was proportional to the water flow rate. This output was transmitted to a strip chart recorder in the model mine control room for continuous monitoring of the water flow rate during each test.

A pressure transducer was installed at each spray manifold on the miner to measure nozzle operating pressure. These transducers produced electrical output signals proportional to the water pressure. This output was directed into the strip chart recorder in the control room for continuous monitoring. Pressure regulators were installed in the water supply line to provide control for obtaining the desired nozzle operating pressures. A booster pump was used throughout this test program to supply the necessary water quantity and pressure to the miner water sprays.

TEST PROCEDURES AND EQUIPMENT

A series of tests were conducted to evaluate the effect of changing water quantity, water pressure, and air quantity on the dust levels at the miner operator's location and in the return. The range of interest for these control parameters was 15 to 35 gpm, 80 to 200 psi, and 3,000 to 9,000 cfm. Tests were to be conducted at the low and high levels and also, at the midrange level for each control parameter. Tests were also to be conducted in the box and slab cut position, with three replicates for each test condition. This would require 162 tests to fulfill the above criteria. To reduce the required number of tests while still obtaining the desired information, a face-centered-cube experimental design was adopted. This limited the test conditions to those shown in table 1 and reduced the number of tests to 102.

In order to fulfill the water application needs specified in the test plan, four different sizes of spray nozzles were selected. Spraying Systems Company BD2, BD3, BD5, and BD8 hollow-cone spray nozzles were used as needed to obtain the desired water flow and pressure combinations.

A hand-held vane anemometer was used to measure the air velocity at the inby end of the return line brattice in order to determine the face air quantity. Adjustments to the return regulator were made as needed to obtain the desired quantity.

Gravimetric dust samplers, operated at 2.0 liters per minute (1/min), were used to sample respirable dust concentrations in the operator's cab and in the return. These

Table No. 1

LEVELS OF CONTROL PARAMETERS TESTED

Water Flow	Water Pressure	Air Flow
15 gpm	80 psi	3,000 cfm
15 gpm	80 psi	9,000 cfm
15 gpm	140 psi	6,000 cfm
15 gpm	200 psi	3,000 cfm
15 gpm	200 psi	9,000 cfm
25 gpm	80 psi	6,000 cfm
25 gpm	140 psi	3,000 cfm
25 gpm	140 psi	6,000 cfm
25 gpm	200 psi	6,000 cfm
35 gpm	80 psi	3,000 cfm
35 gpm	80 psi	9,000 cfm
35 gpm	140 psi	6,000 cfm
35 gpm	200 psi	3,000 cfm
35 gpm	200 psi	9,000 cfm

samplers were operated with 10 millimeter (mm) cyclone preseparators and 37 mm diameter filter cassettes. For each test, two gravimetric samples were collected in the operator's cab and six samples were collected behind the return curtain. Return samples were located in groups of two at approximately 20, 40, and 60 in. (0.51, 1.02, and 1.52 m) from the roof.

Real-time Aerosol Monitors (RAM) were the instantaneous instruments used to supplement the gravimetric samplers. Each RAM is equipped with an internal pump to draw air through a 10 mm cyclone preseparators at a flow rate of 2.0 l/min. The dust laden air passes through a light source and the amount of light deflection is representative of the dust concentration. These dust concentrations were stored in data loggers for later analysis on a computer. A RAM was positioned at each of the four gravimetric sampling positions.

The RAM samplers were operated concurrently with the gravimetric samplers during each two-hour test. In addition, the RAM samplers were operated during a 15 min "base period" before the start of each test. Prior to the base period, the face ventilation had been set, the dust injection system started and the dust cloud allowed to stabilize. The RAM samplers were then used to record the base dust concentrations over a 15 min period, as a means of monitoring fluctuations in the dust feed before any water sprays were operated.

After each test, the net dust weight and sampling time for each gravimetric filter were used to calculate the average dust concentration for the test. The individual concentrations for the six return samples were averaged together to obtain a single return concentration. Likewise, the two dust concentrations from the operator's cab were averaged.

Logger data was downloaded onto a personal computer and analyzed to calculate average dust concentrations for the base and test periods. The base concentrations from the return were used to normalize the gravimetric dust concentrations from each test.

DATA ANALYSIS

The normalized gravimetric dust concentrations from the replicates conducted for each test condition were used to calculate the average dust concentrations that are provided in table 2. These average concentrations represent a wide range of dust levels for the various conditions tested, indicating the test parameters had a substantial impact on resulting dust levels. Since differences were observed from one sampling location to another, each sampling location will be evaluated on an

Table No. 2

AVERAGE GRAVIMETRIC DUST CONCENTRATIONS

WATER FLOW	AIR FLOW	AVERAGE DUST CONCENTRATIONS mg/m ³				
		OPERATOR	RETURN	BOX	SLAB	
GPM	PSI	CFM	BOX	SLAB	BOX	SLAB
15	80	3,000	8.20	2.25	27.7	20.1
15	80	9,000	0.23	0.02	11.8	11.6
15	140	6,000	0.63	1.88	12.2	13.0
15	200	3,000	6.03	6.12	14.6	13.7
15	200	9,000	0.06	0.02	7.2	10.7
25	80	6,000	0.22	1.27	14.3	14.6
25	140	3,000	2.65	3.11	14.6	14.1
25	140	6,000	0.30	0.38	11.0	11.5
25	140	9,000	0.14	0.02	8.2	9.8
25	200	6,000	0.50	0.60	10.7	9.8
35	80	3,000	7.76	2.38	18.6	17.0
35	80	9,000	0.13	0.05	8.9	11.3
35	140	6,000	0.47	0.38	10.5	9.4
35	200	3,000	4.79	0.70	11.6	8.8
35	200	9,000	0.25	0.30	8.0	7.2

individual basis. Multiple regression analysis was used to define the relationship between dust levels and control parameters. Because curvature effects and interactions between the test parameters were suspected, a second-order polynomial was fitted to the data.

Often when fitting a polynomial to data, a high correlation between the linear and squared terms exists and can cause computational difficulties. As a result, a data transformation for the independent variables was made. The difference between each individual test value and the mean value for that test parameter was calculated and used as input data for the regression analysis. For example, rather than using 15, 25, or 35 gpm as an input for the water flow variable, the data was transformed as described (i.e., $15 - 25 = -10$) and -10, 0, or 10 would be used as input. This transformation substantially reduced the correlation between the terms used in the polynomial model. Also, to have all parameters relatively equal in magnitude, the airflow data was rescaled to a range of 30 to 90 rather than 3,000 to 9,000 cfm.

The response surface for the second-order model with three independent variables is defined as:

$$E[Y] = b_0 + b_1x_1 + b_2x_2 + b_3x_3 + b_{12}x_1x_2 + b_{13}x_1x_3 + b_{23}x_2x_3 + b_{11}x_1^2 + b_{22}x_2^2 + b_{33}x_3^2 \quad (1)$$

Typically, when fitting polynomials, the full model may not be needed and those terms that are not significant can be excluded from the model. A stepwise regression procedure determined which terms were significant for each sampling location. The following equations and corresponding adjusted coefficients of multiple determination were obtained:

RIGHT OPERATOR

$$\text{Box Cut: } Y = -0.15284 - 0.00858p - 0.09663c + 0.00035pc + 0.00897g^2 + 0.00023p^2 + 0.00213c^2 \quad (2)$$

$$(R^2_a = 0.87)$$

$$\text{Slab Cut: } Y = 0.72260 - 0.06843g - 0.04694c - 0.00112gp + 0.00231gc + 0.00087c^2 \quad (3)$$

$$(R^2_a = 0.68)$$

RETURN

$$\text{Box Cut: } Y = 11.20004 - 0.16987g - 0.04729p - 0.14346c + 0.00218gp + 0.00481gc + 0.00102pc + 0.00058p^2 \quad (4)$$

$$(R^2_a = 0.85)$$

$$\text{Slab Cut: } Y = 11.42310 - 0.16704g - 0.04063p - 0.07635c - 0.00098gp + 0.00191gc + 0.00064pc + 0.00031p^2 \quad (5)$$

$$(R^2_a = 0.84)$$

where: Y = dust level, mg/m^3
 g = water flow, -10 to 10 gpm
 p = water pressure, -60 to 60 psi
 c = airflow, -30 to 30 cfm*100

These equations indicate that not all parameters are significant for each sampling location. However, all of the equations do have interaction and quadratic terms present.

The coefficient of multiple determination (R^2) is an indication of the proportionate reduction of the total variation in Y that is explained by the independent variables that are included in the model. A value of 1.0 would indicate that a perfect correlation exists and that all observations fall directly on the fitted response surface. The adjusted coefficient of multiple determination (R^2_a) utilizes the number of independent variables in the model in its calculation and provides a more realistic evaluation of the impact of adding variables to a model. All sampling locations but the operator position in the slab cut had an R^2_a greater than or equal to 0.84, indicating that at least 84% of the variation in the observed dust levels is explained by the independent variables included in the model. The data from the operator location in the slab cut was more variable, thus a lower correlation could be expected.

After each model was developed, analysis of the residuals was conducted to determine if the model was a valid representation. Graphical analysis of the residuals indicated that all models were appropriate.

A transformation was then conducted to convert the models into the forms needed to accept the original control parameter levels. This transformation resulted in the following:

RIGHT OPERATOR

$$\text{Box Cut: } Y = 27.48569 - 0.4485g - 0.09282p - 0.40119c + 0.00035pc + 0.00897g^2 + 0.00023p^2 + 0.00213c^2 \quad (6)$$

$$\text{Slab Cut: } Y = 7.92744 - 0.05055g + 0.02798p - 0.20892c - 0.00112gp + 0.00231gc + 0.00087c^2 \quad (7)$$

RETURN

$$\text{Box Cut: } Y = 65.44306 - 0.76405g - 0.32497p - 0.40689c + 0.00218gp + 0.00481gc + 0.00102pc + 0.00058p^2 \quad (8)$$

$$\text{Slab Cut: } Y = 36.73387 - 0.14400g - 0.14109p - 0.21372c - 0.00098gp + 0.00191gc + 0.00064pc + 0.00031p^2 \quad (9)$$

where: Y = dust level, mg/m^3

g = water flow, 15 - 35 gpm

p = water pressure, 80 - 200 psi

c = airflow, 30 - 90 cfm*100

These equations were used to construct response surface plots and contour plots for each sampling location. The results will be presented and discussed.

Operator Position

Figure 2 shows the response surface plot constructed from the right operator, box cut model with the water flow held constant at 15 gpm ($0.057 \text{ m}^3/\text{min}$). This plot illustrates the impact of increasing air flow and water pressure and shows the curvature that is present in the relationship. As illustrated, increases in air quantity results in reduced dust levels until airflow exceeds 8,000 cfm ($3.78 \text{ m}^3/\text{sec}$). Increasing the water pressure results in reduced dust levels only to around 140 psi (9.84 kg/cm^2), then the dust levels begin to rise. The increases in dust levels probably result from undesirable airflow turbulence created by the high airflow and additional dust rollback caused by the higher water pressures (Foster-Miller Inc., 1985). The point at which additional increases in control parameters no longer result in corresponding decreases in dust concentration is referred to as the 'point of diminishing return'. This point should be identified to minimize water and air usage while maximizing dust control.

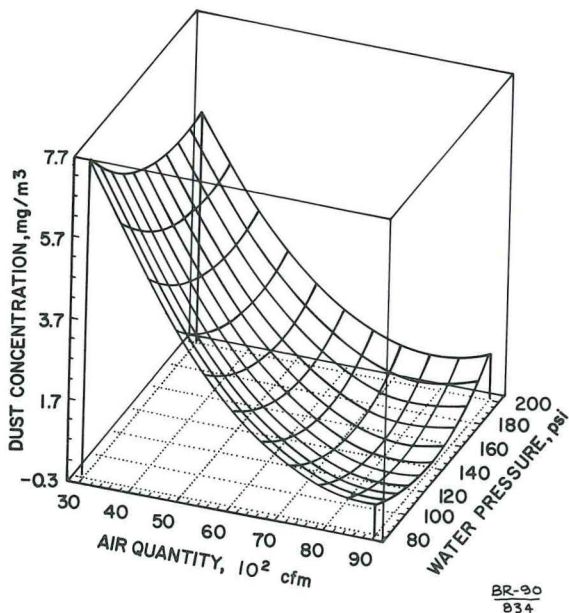


FIGURE 2. Response surface plot of predicted operator dust levels in the box cut at 15 gpm.

Filters with dust weights too low to be measured by the balance were obtained for some higher airflow conditions and resulted in average dust concentrations as low as 0.02 mg/m^3 in table 2. The inclusion of these values as input for the multiple regression analysis caused some of the model-predicted dust levels for high airflows to be negative. Negative dust levels cannot occur but were reported in this case to illustrate trends.

To more readily identify the point of diminishing return, contour plots were produced. Figure 3 contains the contour plot for the right operator, box cut model at a constant water flow of 15 gpm ($0.057 \text{ m}^3/\text{min}$). Minimum dust levels can be obtained for different conditions. For example, near 7,000 cfm ($3.30 \text{ m}^3/\text{sec}$), the dust levels decrease until approximately 140 psi (9.84 kg/cm^2) is reached and then the dust levels remain constant before increasing. However, near 3,000 cfm ($1.42 \text{ m}^3/\text{sec}$), the dust level continues to decrease up to approximately 160 psi (11.25 kg/cm^2). The interaction between water pressure and airflow accounts for the shift in effectiveness at different water pressures. Similarly, with increasing airflow, dust levels continue to decrease until approximately 8,400 cfm ($3.96 \text{ m}^3/\text{sec}$) is reached. Apparently, at higher air quantities, undesirable airflow patterns may be forming to carry dust to the operator. Similar dust contours were found for higher water flows conditions.

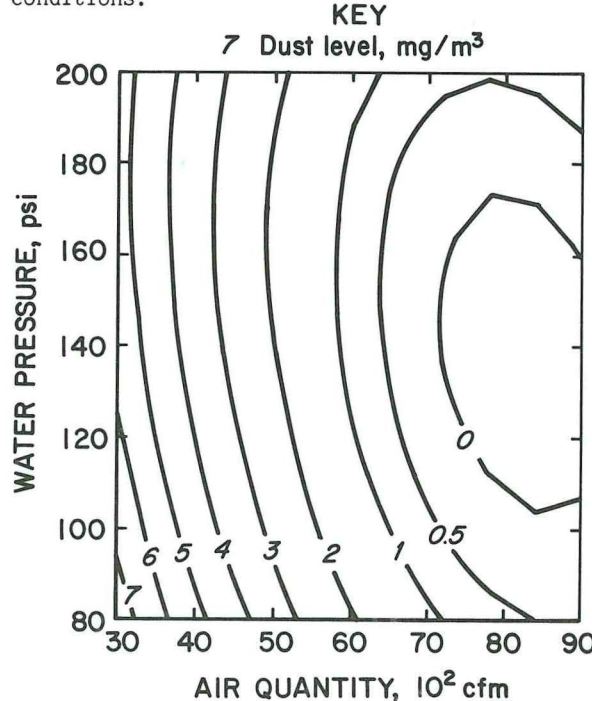


FIGURE 3. Contour plot of predicted operator dust levels in the box cut at 15 gpm.

Contour plots were constructed with the water pressure held constant to determine the impact

of water flow on dust levels. Figure 4 illustrates the dust levels found at the operator location with the water pressure constant at 80 psi (5.62 kg/cm²). The patterns present in this figure are quite similar to those found for constant water flow. In this case, approximately 25 gpm (0.095 m³/min) resulted in minimized dust levels.

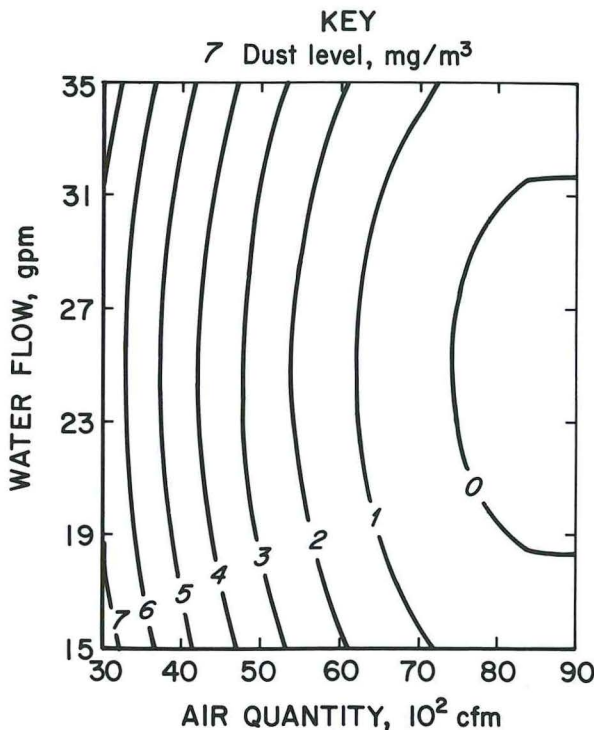


FIGURE 4. Contour plot of predicted operator dust levels in the box cut at 80 psi.

As a result, one could limit the use of water to approximately 25 gpm and 140 psi (9.84 kg/cm²) and still achieve maximum dust reduction for the system tested. Increases in airflow up to 8,400 cfm (3.96 m³/sec) would result in improvements in dust exposure at the operator.

The effect of control parameter interaction was much more pronounced for the operator position in the slab cut. Figures 5, 6, and 7 are the response surface plots for constant flow rates of 15, 25, and 35 gpm conditions, respectively. These plots show how the plane of dust levels completely reverses when going from low to high water flows. Increases in water pressure result in increases in dust at 15 gpm, no impact on dust at 25 gpm, and reductions in dust at 35 gpm.

The dust levels observed at the operator position in the slab cut over the range of airflows are also somewhat different to that found in the box cut. Increases in airflow resulted in reductions in dust levels in all

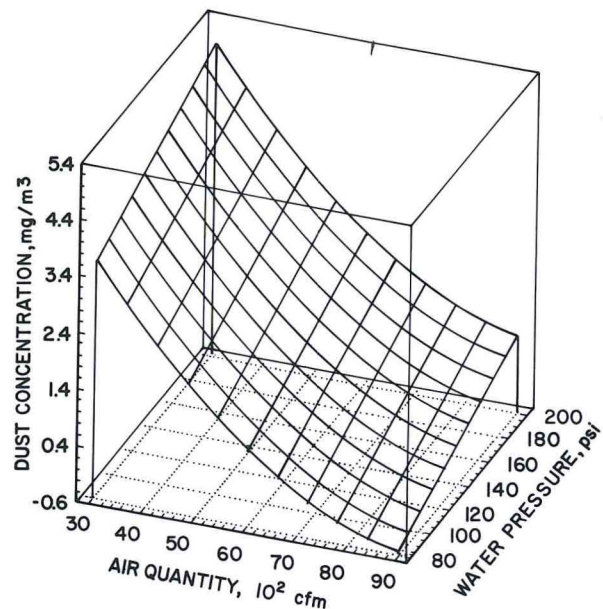


FIGURE 5. Response surface plot of predicted operator dust levels in the slab cut at 15 gpm.

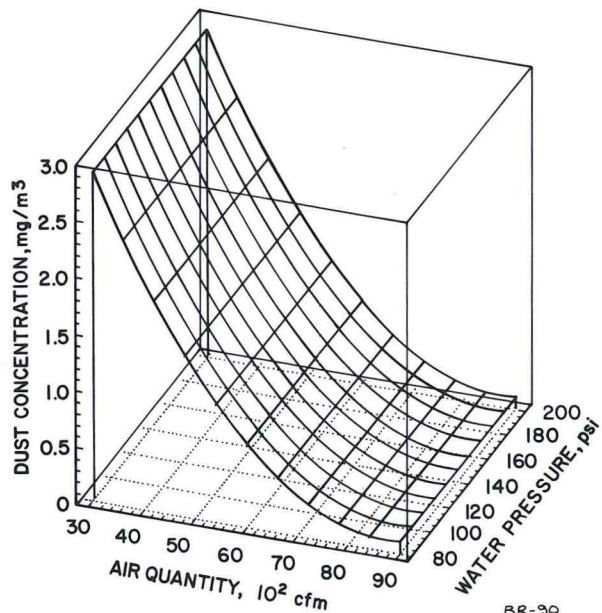


FIGURE 6. Response surface plot of predicted operator dust levels in the slab cut at 25 gpm.

cases except for 35 gpm water flow. At approximately 7,000 cfm (3.30 m³/sec), additional increases in the air quantity aggravated operator dust exposure.

For the slab cut, the operator's cab was positioned closer to the corner of the crosscut where less consistent airflow patterns were more likely. Also, the width of the slab cut resulted in approximately half of the water

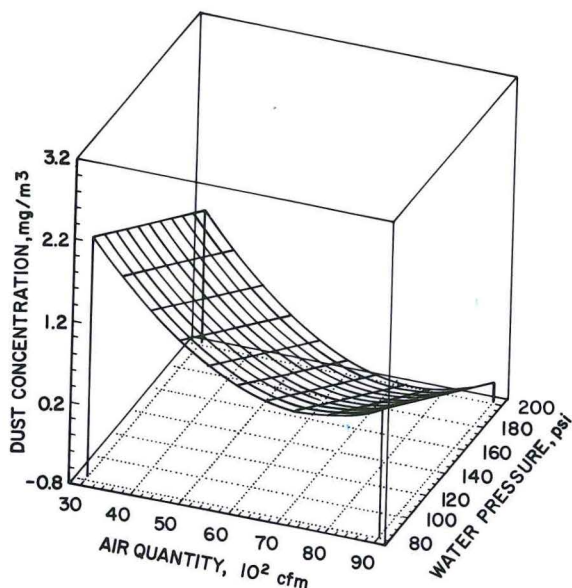


FIGURE 7. Response surface plot of predicted operator dust levels in the slab cut at 35 gpm.

sprays impacting against the face, while the other sprays discharged into the open box cut. Thus, face airflow patterns different from those present in the box cut were expected. These factors contributed to varying face airflow patterns and turbulence that effected the dust levels at the operator's position.

Due to the interaction taking place, a unique point of diminishing return was not found for the operator position in the slab cut. For each level of water flow, a different combination of control parameters produced the lowest dust levels. Table 3 provides a summary of the predicted dust concentrations calculated for both the slab and box cuts for the low, middle, and high level combinations of the

control parameters. The data offers insight about which combinations of control parameters provide the greatest dust reductions.

Return Position

The dust reductions found for the return sampling position generally followed a more consistent trend for both the box and slab cut locations, particularly at lower water flows. Figures 8 and 9 show the response surface plots for the box and slab cuts at a constant water flow of 15 gpm ($0.057 \text{ m}^3/\text{min}$). Although the magnitude of the dust levels differs, the shape of each response surface is similar. Examination of the contour plots, figures 10 and 11, further confirm the same dust trends are found for both cuts.

Return dust concentrations predicted by the regression models are listed in table 4. Airflow appears to be the most significant individual control parameter. Increases in airflow resulted in decreases in dust levels throughout the range tested, with a maximum reduction of 57% in the box cut when comparing results at 3,000 cfm ($1.42 \text{ m}^3/\text{sec}$) to those at 9,000 cfm ($4.25 \text{ m}^3/\text{sec}$).

The continued improvement achieved with airflow in the return location, when compared to the operator position, is due to the method by which airflow controls dust at each location. For increases in airflow at the return location, dust reductions result from greater dilution of the dust cloud. At the operator's position, increased airflow also offers greater dilution but the primary dust control appears to come from reducing rollback.

For the 15 gpm level, water pressure interaction with air quantity was present so that the point of diminishing return was not constant. At lower air velocities, higher water pressures continued to be effective, but as the air quantity was raised, increases in water

Table No. 3

SUMMARY OF PREDICTED DUST CONCENTRATIONS FOR THE OPERATOR SAMPLING LOCATION

BOX CUT

	15 gpm			25 gpm			35 gpm		
	80 psi	140 psi	200 psi	80 psi	140 psi	200 psi	80 psi	140 psi	200 psi
3,000 cfm	7.52	5.56	5.21	6.62	4.66	4.32	7.52	5.56	5.21
6,000 cfm	2.07	0.74	1.04	1.17	-0.15	0.14	2.07	0.74	1.04
9,000 cfm	0.44	-0.24	0.69	-0.45	-1.14	-0.21	0.44	-0.24	0.69

SLAB CUT

	15 gpm			25 gpm			35 gpm		
	80 psi	140 psi	200 psi	80 psi	140 psi	200 psi	80 psi	140 psi	200 psi
3,000 cfm	3.62	4.29	4.96	2.91	2.91	2.91	2.21	1.53	0.86
6,000 cfm	0.74	1.41	2.08	0.72	0.72	0.72	0.71	0.04	-0.63
9,000 cfm	-0.59	0.09	0.76	0.10	0.10	0.10	0.78	0.11	-0.57

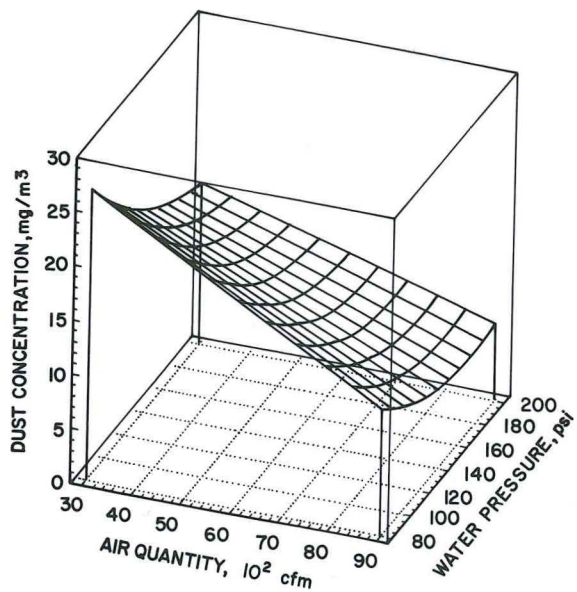


FIGURE 8. Response surface plot of predicted return dust levels in the box cut at 15 gpm.

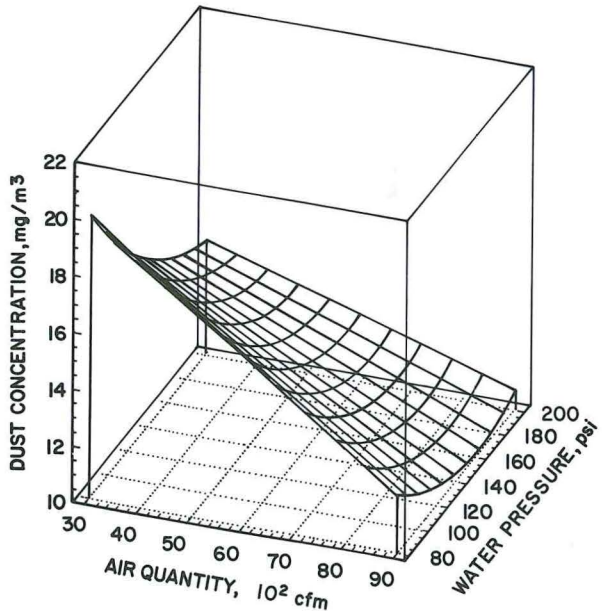


FIGURE 9. Response surface plot of predicted return dust levels in the slab cut at 15 gpm.

pressure became ineffective. For example, at 3,000 cfm, dust reductions were realized over the 80 - 200 psi ($5.62-14.06 \text{ kg/cm}^2$) range, but at 8,000 cfm ($3.78 \text{ m}^3/\text{sec}$), reductions in dust levels ceased at approximately 170 psi (11.95 kg/cm^2). Similar findings were observed for higher water flow levels.

Figures 12 and 13 show the response surface plots for the box and slab cuts at a constant water pressure of 80 psi. These plots show that

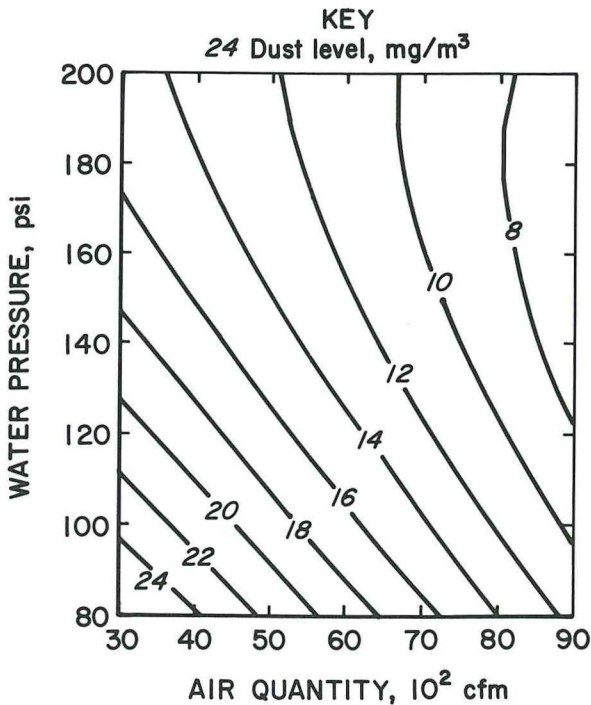


FIGURE 10. Contour plot of predicted return dust levels in the box cut at 15 gpm.

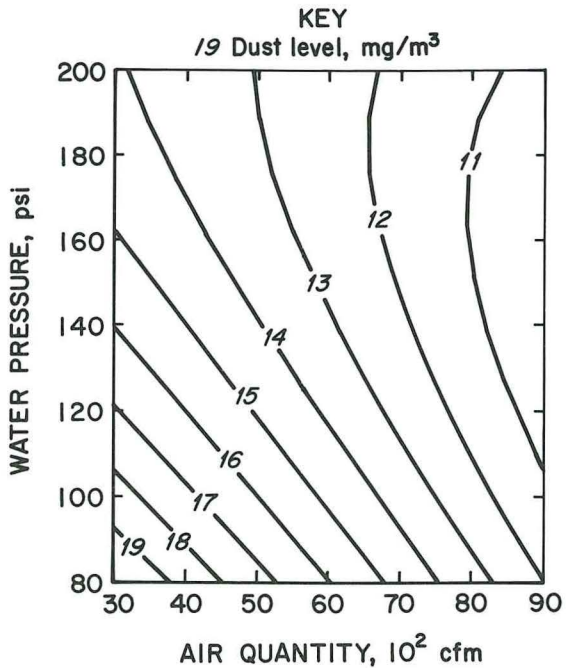


FIGURE 11. Contour plot of predicted return dust levels in the slab cut at 15 gpm.

increased water flow reduces dust levels but not at a very significant rate, particularly when compared to the improvement made by increasing airflow. These plots reinforce the finding that

Table No. 4

SUMMARY OF PREDICTED DUST CONCENTRATIONS FOR THE RETURN SAMPLING LOCATION

BOX CUT

	15 gpm			25 gpm			35 gpm		
	80 psi	140 psi	200 psi	80 psi	140 psi	200 psi	80 psi	140 psi	200 psi
3,000 cfm	26.71	18.65	14.74	22.26	15.50	12.91	17.81	12.36	11.07
6,000 cfm	19.13	12.90	10.83	16.12	11.20	10.44	13.11	9.50	10.05
9,000 cfm	11.54	7.15	6.93	9.97	6.90	7.98	8.41	6.64	9.03

SLAB CUT

	15 gpm			25 gpm			35 gpm		
	80 psi	140 psi	200 psi	80 psi	140 psi	200 psi	80 psi	140 psi	200 psi
3,000 cfm	20.07	15.96	14.06	18.42	13.71	11.23	16.76	11.47	8.40
6,000 cfm	16.06	13.09	12.36	14.97	11.42	10.10	13.89	9.75	7.84
9,000 cfm	12.04	10.23	10.65	11.53	9.13	8.96	11.02	8.03	7.27

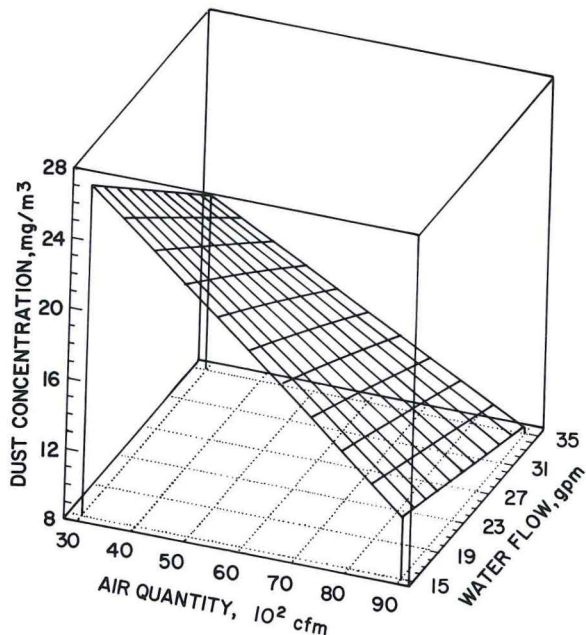


FIGURE 12. Response surface plot predicted of return dust levels in the box cut at 80 psi.

airflow has the most significant impact on dust levels and that less dramatic changes are realized with water flow.

CONCLUSIONS

Results of these tests show that airflow has the potential to make the most substantial individual reductions in dust concentrations at both the operator (99%) and return locations (57%). These reductions can be attributed to overall dilution of the dust cloud and the prevention of rollback at the operator location. Undesirable airflow turbulence resulted in increased dust levels at the operator location

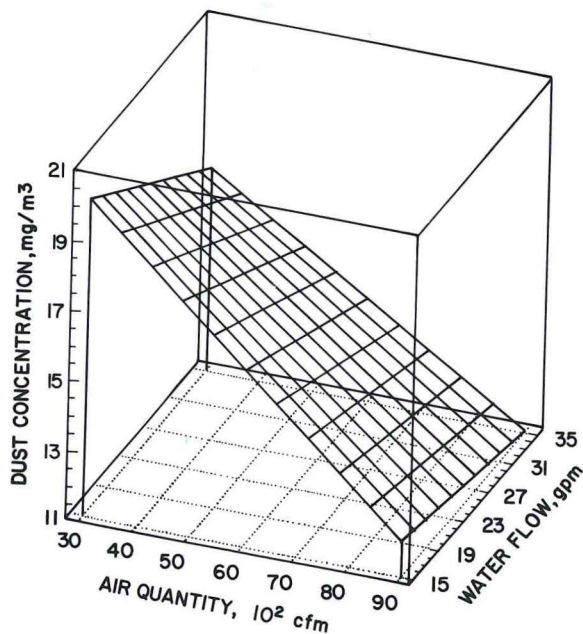


FIGURE 13. Response surface plot of predicted return dust levels in the slab cut at 80 psi.

at some high airflows. However, these increases only occurred at airflows above 7,000 cfm ($3.30 \text{ m}^3/\text{sec}$).

Water pressure was shown to have a significant impact on dust levels, particularly at the operator's position. If the water pressure was too high, increased rollback was observed, primarily at the lower airflows tested. It is suspected that many continuous miner sections operate in the lower half of the airflow range tested and would therefore be more susceptible to rollback induced by high water pressures. Therefore, the potential for aggravating dust levels must be considered and

onsite testing should be conducted if water pressures above 140 psi (9.84 kg/cm²) are desired.

Water quantity had the least impact on reducing operator or return dust levels. Generally, increases above 25 gpm (0.095 m³/min) offered little improvement in dust control. However, our test setup did not take into consideration another area where increased water flow should have additional benefits. No provisions were available to simulate the dust liberation which could occur from coal transfer from the miner conveyor into a shuttle car. Any dust generated by this operation, has the potential to be carried to the miner operator's location. In this situation, one could surmise that increased water application while cutting may reduce the dust liberation during transfer, as a result of a wetter coal product.

Interaction between control parameters was prevalent throughout the test series. Often, the point of diminishing return for one control parameter was dependent on the level of another control parameter. With such interaction present, the level of application for two of the three parameters tested must be known to determine the desired level of the third parameter. In light of these interactions, the calculated regression models would be useful in selecting possible alternatives for reducing dust levels. Results also confirmed that application of control parameters at particular levels may significantly benefit one sampling

location (return) but adversely impact another location (miner operator). The area of concern for the mine operator must be considered when selecting application levels for these dust control parameters. If a mine has personnel working downstream of the miner, one set of control parameters may be more suitable than those selected for a mine that has the operator out of compliance.

It is apparent that application of airflow and water is not a straightforward undertaking. For mining conditions simulated by the laboratory study, increases in airflow to 8,400 cfm (3.96 m³/sec), in water pressure to 140 psi (9.84 kg/cm²), and in water quantity to 25 gpm (0.095 m³/min) typically offer continuing improvement in dust control at the operator and return locations.

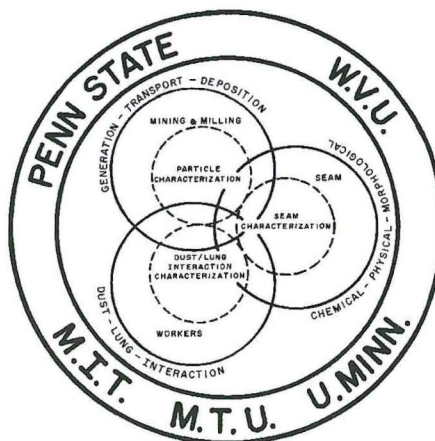
REFERENCES

Improved Diffuser and Sprayfan Systems for Ventilation of Coal Mine Working Faces (contract J0113010), Foster-Miller Inc., July 1985; NTIS PB 86-168440.

Ramani, R. V., et al., 1987, "Fundamental Studies on the Relationship Between Quartz Levels in the Host Material and the Respirable Dust Generated During Mining," Volume I: Experiments, Results and Analyses (contract H0358031), PA State Univ. BuMines OFR 36-88, 179 pp; NTIS PB 88-214325.

3rd SYMPOSIUM ON RESPIRABLE DUST IN THE MINERAL INDUSTRIES

Edited by
ROBERT L. FRANTZ
and
RAJA V. RAMANI



Published by
Society for Mining, Metallurgy, and Exploration, Inc.
Littleton, Colorado • 1991

TN312
• I61
1990

Copyright © 1991 by the
Society for Mining, Metallurgy, and Exploration, Inc.

Printed in the United States of America by
Cushing-Malloy, Inc., Ann Arbor, MI

All rights reserved. This book, or parts thereof, may not be
reproduced in any form without permission of the publisher.

Library of Congress Catalog Card Number 91-66952
ISBN 0-87335-098-7

RESPIRABLE DUST IN THE MINERAL INDUSTRIES

Proceedings of the 3rd Symposium on Respirable Dust
in the Mineral Industries
October 17-19, 1990
Pittsburgh, PA

Sponsored by

The Generic Mineral Technology Center for Respirable Dust
The Pennsylvania State University
West Virginia University
University of Minnesota
Massachusetts Institute of Technology
United States Bureau of Mines (USBM)
Mine Safety and Health Administration (MSHA)
National Institute for Occupational Safety and Health (NIOSH)
American Conference of Governmental Industrial Hygienists (ACGIH)